JOURNAL OF ORAL MICROBIOLOGY
2023, VOL. 15, 2204250
https://doi.org/10.1080/20002297.2023.2204250

Taylor & Francis
Taylor & Francis Group

ORIGINAL ARTICLE

OPEN ACCESS Check for updates

Exopolysaccharides metabolism and cariogenesis of *Streptococcus mutans* biofilm regulated by antisense *vicK* RNA

Yuting Sun[a,b,c†], Hong Chen[a,b,c†], Mengmeng Xu[a,b,c], Liwen He[a,b,c], Hongchen Mao[a,b,c], Shiyao Yang[a,b,c], Xin Qiao[a,b,c] and Deqin Yang[a,b,c]

[a]Department of Endodontics, Stomatological Hospital of Chongqing Medical University, Chongqing, China; [b]Chongqing Key Laboratory of Oral Diseases and Biomedical Sciences, Chongqing, China; [c]Chongqing Municipal Key Laboratory of Oral Biomedical Engineering of Higher Education, Chongqing, China

ABSTRACT

Background: *Streptococcus mutans* (*S. mutans*) is a pivotal cariogenic pathogen contributing to its multiple virulence factors, one of which is synthesizing exopolysaccharides (EPS). VicK, a sensor histidine kinase, plays a major role in regulating genes associated with EPS synthesis and adhesion. Here we first identified an antisense *vicK* RNA (AS*vicK*) bound with *vicK* into double-stranded RNA (dsRNA).
Objective: This study aims to investigate the effect and mechanism of AS*vicK* in the EPS metabolism and cariogenesis of *S. mutans*.
Methods: The phenotypes of biofilm were detected by scanning electron microscopy (SEM), gas chromatography-mass spectrometery (GC-MS) , gel permeation chromatography (GPC) , transcriptome analysis and Western blot. Co-immunoprecipitation (Co-ip) assay and enzyme activity experiment were adopted to investigate the mechanism of AS*vicK* regulation. Caries animal models were developed to study the relationship between AS*vicK* and cariogenicity of *S. mutans*.
Results: Overexpression of AS*vicK* can inhibit the growth of biofilm, reduce the production of EPS and alter genes and protein related to EPS metabolism. AS*vicK* can adsorb RNase III to regulate *vicK* and affect the cariogenicity of *S. mutans*.
Conclusions: AS*vicK* regulates *vicK* at the transcriptional and post-transcriptional levels, effectively inhibits EPS synthesis and biofilm formation and reduces its cariogenicity *in vivo*.

ARTICLE HISTORY
Received 19 December 2022
Revised 10 April 2023
Accepted 13 April 2023

KEYWORDS
Streptococcus mutans; Antisense RNA; *vicK* gene; biofilm growth; exopolysaccharides; dental caries; bacterial genetics

Introduction

Dental caries is a destructive disease causing demineralization of hard tissues chronically, eventually leading to cavities. It is an enormous health problem worldwide among the most prevalent diseases and greatly reduces the quality of life for those affected [1,2]. Dental caries arises from dental plaque composed of EPS and other matrix [3]. The oral cavity is a habitat for diverse microorganisms, which are associated with the health and disease state of the host. *S. mutans*, one of the primary etiological agents of dental caries, resides within biofilm of dental plaque. As with many cariogenic pathogens, the virulence of it depends in part on the resistance to acid and the metabolism of diet-derived carbohydrates accompanied by the production of acid and EPS [4].

It is clear that inhibition of EPS synthesis in dental plaque biofilm is the key to attenuate virulence of *S. mutans*. EPS not only promotes its adhesion through a sucrose-dependent pathway but also provides nutrients and enhances bacterial tolerance [5]. It can dynamically regulate pathogenic microecology and affect biofilm formation and stability [6,7]. EPS can also affect the diffusion of lactic acid, resulting in an acidic microenvironment on the tooth surface. The mechanisms by which lactic acid affects the virulence factors of *S. mutans* are complex and diverse. *S. mutans* metabolizes dietary sugars through lactate dehydrogenase (LDH), catalyzes pyruvate to produce lactate, reduces the pH value of plaque and affects its acid tolerance response (ATR) [8,9]. The formation of EPS mainly involves glucosyltransferases (GTFs), fructosyltransferases (Ftfs), and glucan-binding proteins (GBPs). GTFs enzymatically decompose sucrose into glucose and fructose, which are then assembles glucose through glycosidic bonds to form EPS. Ftf converts sucrose to fructan, which functions as an extracellular storage compound [10]. GBPs can promote the binding of bacterial glucans, mediate bacterial sucrose-dependent adhesion, and promote biofilm

CONTACT Deqin Yang yangdeqin@hospital.cqmu.edu.cn Department of Endodontics, Stomatological Hospital of Chongqing Medical University, Chongqing 4404100, China
†The author contributed equally to this work.
Supplemental data for this article can be accessed online at https://doi.org/10.1080/20002297.2023.2204250

formation [11,12]. EPS in *S. mutans* is principally glucan, including water-insoluble glucan (WIG) and water-soluble glucan (WSG), synthesized by Gtfs and decomposed by dextranase (Dex) [7,13]. Therefore, numerous studies have been focused on exploring methods of inhibiting synthesis and promoting digestion of EPS, which is an effective strategy of caries prevention and treatment. In gram-positive bacteria, the VicRK (WalRK or YycFG) two-component signal transduction system (TCS) is essential for diverse vital cellular processes, such as membrane homeostasis, bacterial virulence, biofilm formation and cell division [14–16]. Vick, namely, a sensor histidine kinase, can initiate a histidine autophosphorylation upon external stimuli and transmit the phosphorylation signal to VicR, which positively modulates downstream gene associated with polysaccharide metabolism [17,18]. Numerous studies [17,19,20] have been focused on exploring methods of inhibiting synthesis EPS based on the VicRK two-component signal transduction system; however, the regulatory pathway of *vicK* gene is still vague. In addition, VicK can also influence GcrR, also known as CovR, which is an orphan response regulator [21]. It is a negative transcriptional regulator associated with stress tolerance responses related to the ATR mechanism [22] and regulation of bacterial biofilms. GcrR can also bind to the promoter regions of *gtfB* and *gtfC* to regulate sucrose-dependent adhesion.

Gene expression is controlled by bacteria with a complex network regulatory mechanism, and non-coding RNAs (ncRNAs) are the key regulators. Antisense RNAs (asRNAs) are a class of non-coding RNAs that are transcribed from opposite strands of their target genes. AsRNAs typically bind to target mRNA to form dsRNA in a completely complementary manner without companion proteins to maintain stability and function [23]. This progress has advantages in terms of accurate and flexible rapid gene regulation, which is essential for bacteria to adapt to host immune response [24,25].

Degradation of RNA is a crucial mechanism for regulating gene expression in organisms. *Rnc*, located upstream of *vicR*/*K*/*X*, affects *vicR*/*K*/*X* gene at the post-transcriptional level [19]. In previous studies, we found that *rnc* gene regulates carbohydrate transport and metabolism of *S. mutans* by regulating the expression of ncRNAs (AS*vicR* and msRNA1657). In addition, RNAse III, encoded by *rnc*, is a widespread endoribonuclease that binds and cleaves dsRNA. AsRNA allows precise control of the regulatory circuit, which is the key for bacteria to quickly adapt to environmental changes [26,27]. Plenty of studies have confirmed that the virulence factors and adaptability of *S. mutans* can be regulated by asRNAs, indicating the feasibility of regulating protein function by asRNAs to affect its cariogenesis [28,29].

Previous studies have explored *vicK* mutant strains, but the upstream regulation of it is still vague. In addition, regulating AsRNA generally has advantages over regulating proteins because they require less energy to synthesize and act quickly, which is the key for bacteria to quickly adapt to the host immune response. Therefore, we analyzed the RNA-seq transcriptional sequencing results of *rnc* deletion strain and standard strain UA159. An asRNA termed AS*vicK* with high expression in *rnc* deletion strain was first found and studied. We found that AS*vicK* could effectively inhibit the expression of *vicK* through binding with *vicK* into ds RNA. In this study, we investigate whether AS*vicK* play a role in EPS metabolism and biofilm formation. We also sought to explore the potential molecular mechanism and cariogenesis of AS*vicK* in *S. mutans.*

Materials and methods

Ethics statement and clinical specimens

Clinical strains (Appendix Table 1), for this study, were isolated from SECC patients who originated from the pediatric department of Affiliated Hospital of Stomatology, ChongQing Medical University. This study was approved by the Ethics Committee of the School of Stomatology, Chongqing Medical University. Children, aged from 3 to 5 years were divided into two groups: the CF children group and the SECC children group, as well as were performed dmft score. Dental plaque from the buccal surfaces of anterior teeth and the first mandibular molar was obtained using sterile dental probes and pooled, kept in sterilized tubes containing PBS buffer on ice and transferred to the lab within 2 h. Samples were diluted and plated onto mitis salivarius agar (MSA) (Difco Laboratories, Detroit, USA) supplemented with 0.2 U/ml bacitracin (Sigma Chemical Co, St Louis, USA) and 15% (wt/vol) sucrose. Plates were incubated in an atmosphere of 80% N_2 and 20% CO_2 at 37°C for 48 h. Five colonies were randomly chosen from each sample based on their morphology [20]. Ten CF clinical isolates and 10 SECC strains were involved in the present study and used for RT-qPCR to compare gene expression. Animal experiments were reviewed and approved by the Ethics Committee of the Affiliated Hospital of Stomatology Chongqing Medical University, ChongQing, China (Number of permit: (2022)126).

Bacterial strains and growth conditions

Bacterial strains and plasmids used in this study are listed in Appendix Table 2. The transcription sequencing results of *rnc* mutant strains and the UA159 strain were uploaded in on the website of national center for biotechnology information (NCBI), accession: SRR22348593-SRR22348598. The sequences of AS*vicK* and AS*vicK* with HIS tag are listed in Appendix Figure 1. Sequences of *vicK* were obtained by oligonucleotides synthesis (Sangon Biotech, Shanghai, China) and the promoter sequence was synthesized [30]. The mutant strains were constructed using the shuttle vector pDL278 inserted AS*vicK*, AS*vicK* with HIS tag and *vicK* sequences and transformed into DH5α then extracted and were determined through BamH I and EcoR I enzyme for Gel electrophoresis and sequencing identification (Sangon Biotech, Shanghai, China). For the transformation, the mid-exponential-phase *S. mutans* with the competence stimulating peptide (CSP, 1 μg/mL) and recombinant plasmids were cultured for 3 h in an atmosphere of 80% N_2 and 20% CO_2 at 37°C. The bacterial cultures were plated onto BHI supplemented with spectinomycin (1 mg/mL) and incubated in an atmosphere of 80% N_2 and 20% CO_2 at 37°C for 48 h. Single colonies were screened and subcultured for 48 h. The levels of AS*vicK* and *vicK* expression in the resulting mutants were monitored and compared to its level of expression in UA159 by RT-qPCR.

Unless otherwise specified, *S. mutans* strains were grown overnight in brain heart infusion (BHI) in an atmosphere of 80% N_2 and 20% CO_2 at 37°C. Appropriate antibiotics were added when culturing the mutant strains, i.e. spectinomycin (1 mg/mL) for *vicK* mutans strains. *Escherichia coli* (*E. coli*) was grown aerobically in Luria–Bertani (LB) medium supplemented with ampicillin (100 μg/mL) as needed. The overnight cultures were diluted 20-fold into BHI and grown for 2.5–3 h to mid-logarithmic phase (optical density at 600 nm; OD600 = 0.3) then were determined by the multimode plate reader (PerkinElmer, EnSpire, Singapore).

Isolation of RNA and cDNA reverse transcription

For total RNA extraction, clinical isolates and laboratory strains were grown in BHI in an atmosphere of 80% N_2 and 20% CO_2 at 37°C overnight, then were diluted 20 times in fresh BHI and grown for 2.5–3 h to mid-logazai rithmic phase (OD600 = 0.3). For biofilm of *S. mutans* formation, each well of a 24-well plate, containing 1.5 mL sterile BHI with 1% sucrose, was inoculated with 15 μL of bacteria solution after reached mid-logarithmic phase (OD600 = 0.3). Then incubated strains anaerobically for 24 h. Biofilms were collected with a cell scraper after removing solution with planktonic bacteria and rinsed gently twice with sterile phosphate-buffered saline (PBS). The precipitate was added with 200 μL of red cell lysis buffer while the walls of cells were broken by the freezing grinding apparatus (TuoHe, China). After the cells being homogenized in the 800 μL of RNAiso Plus solution, added 160 μL of chloroform to the homogenate solution, mixed well, and then centrifuged to separate the solution into three layers, the top layer of which was a clear liquid containing RNA. The top liquid layer was removed and pipetted into a new tube, followed by precipitation of total RNA by isopropanol. The purity (A260/A280) and concentration of RNA were determined using a NanoDrop2000 spectrophotometer (Thermo Scientific, Waltham, MA, USA). Elimination of genomic DNA (gDNA) and reverse-transcription reaction with primers (Appendix Table 3) using the PrimeScriptTM RT reagent Kit with gDNA Eraser (TaKaRa, Japan) in accordance with the recommendations of the supplier. All assays were performed in triplicate from at least three different experiments.

Transcription analysis by RT-qPCR

RT-qPCR was carried out with a Bio-Rad Applied Biosystems ABI 7500 System (Bio-Rad Laboratories, Hercules, CA, USA) using the PrimeScriptTM RT reagent Kit with gDNA Eraser (TaKaRa, Japan). The reaction mixture was prepared, 20 μL for each well, containing 10 μL TB Green Premix Ex Taq II (TaKaRa, Japan), 2μL template cDNA, 1 μL 10 μM PCR Forward Primer, 1 μL 10 μM PCR Reverse Primer and 6 μL sterile purified water. Protocol recommended was followed: 95°C, 30 s (initial denaturation), followed by 40 cycles of 95°C for 5 s (denaturation), 60°C for 31 s (primer annealing), then 95°C for 15 s, 60°C for 1 min and 95°C for 15 s (dissociation). After the reaction is complete, check the amplification and melting curves and plot a standard curve if a quantitative assay will be performed. Threshold cycle values (CT) were quantified and the expression of each gene was normalized relative to the expression of the *gyrA* gene, which was used as an internal reference. Data were calculated according to the $2-\Delta\Delta CT$ method [31]. All assays were performed in triplicate from at least three different experiments. The primers used in this study are shown in Appendix Table 3.

Assays of bacterial growth and biofilm structural formation

CV assay, SEM, and CLSM were applied to determine the 24 h biofilms of UA159, AS*vicK*, and SmuvicK+ strains. For detection of bacterial growth curves and colony-forming units (CFUs), strains of UA159, AS*vicK* and SmuvicK+ were cultured anaerobically at 37°C in BHI and were measured the OD values at 600 nm every hour for 20 h at 37°C [32].

Morphological and physiological characteristics of bacterial biofilms, subcultured for 6 h after overnight culture, were observed by SEM. For biofilm of *S. mutans*, strains were grown in BHI while *vicK* mutant strains were grown in BHI with spectinomycin (1 mg/mL) in an atmosphere of 80% N_2 and 20% CO_2 at 37°C overnight, then they were subcultured at

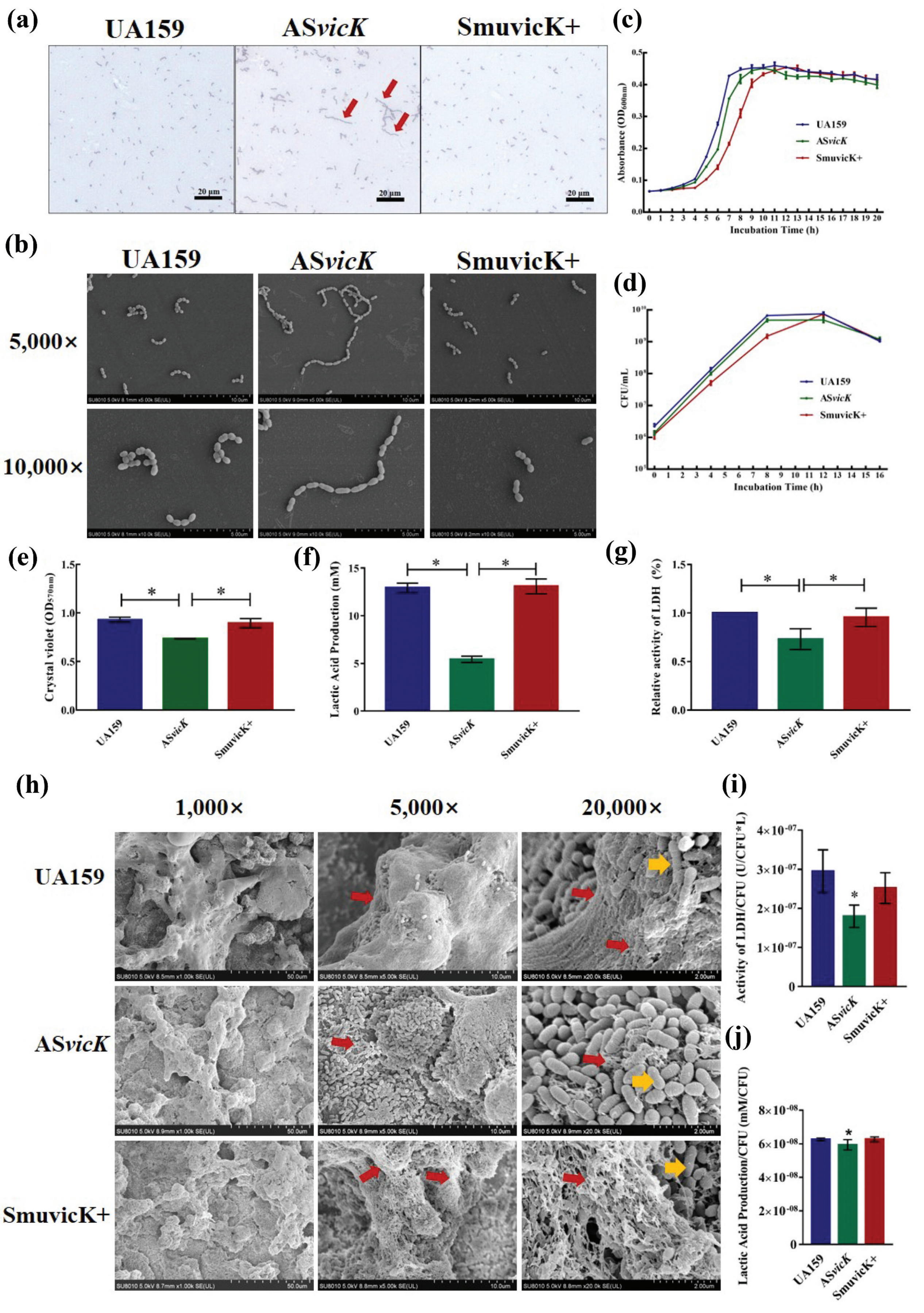

Figure 1. ASvicK altered morphology and growth of bacteria and biofilm. (a) Morphology structure of UA159, AS*vicK* and SmuvicK+. Significant differences were apparent in AS*vicK* strain, which has a longer chain and diverse size and shapes; (b) SEM of UA159, AS*vicK*, and SmuvicK+ cultured in BHI supplemented with 1% sucrose. The AS*vicK* strain appeared longer and diverse cell size and shape; (c) Growth curve of UA159 and the *vicK* mutant strain. The bacteria strains were grown in BHI at 37°C anaerobically and were monitored every hour; (d) CFU curve of UA159 and the *vicK* mutant strain. The bacteria strains were

1:20 in fresh BHI for 2.5–3 h. Each well with a round coverslip of a 24-well plate containing 1.5 mL sterile BHI with 1% sucrose, was inoculated with 15 μL of bacterial solution (OD600 = 0.3) and incubated them anaerobically for 6 h. Then, we removed solution with planktonic bacteria and washed biofilms gently twice with sterile PBS, followed by fixed with 2.5% glutaraldehyde avoiding light at room temperature for 4 h and washed twice again. Serial dehydration included preparations with ethanol solutions (30%, 50%, 75%, 85%, 95% and 99%) every time stood for 15 min, critical-point drying with liquid CO_2, and coating with gold powder. Biofilm specimens were evaluated via scanning electron micrographs we obtained by a SEM (Inspect Hillsboro, OR, USA).

For a mature bacterial biofilm formation, bacterial strains after subcultured reaching the mid-exponential phase (OD600 = 0.3) were inoculated with 15 μL in a 24-well plate in which each well containing 1.5 ml sterile BHI with 1% sucrose and incubated them anaerobically at 37°C for 24 h then they can be used for CLSM and CV.

To assess biomass structure, the EPS matrix of *S. mutans* biofilms was stained with 1 μM Alexa Fluor 647-labeled dextran conjugate (Life Tech, USA), and bacterial cells in the biofilm were labeled with 50 μL Syto9 Nucleic Acid Stain (Life Tech, USA). Next, CLSM (Leica, Solms, Germany) was performed at 63× using an oil-immersion objective lens. Three-dimensional reconstruction of the biofilms as well as imaging biomass quantification was analyzed using Imaris.

The biomasses of biofilms were determined by CV assay. Solution with planktonic bacteria was removed after maturity and the biofilms were washed gently twice with PBS, followed by stained with 500 μL 0.1% (w/v) crystal violet in each well on the orbital shaker for 15 min (100 rpm/min) and removed solution. Afterwards, biofilms were washed twice with PBS and added 1 mL 33% acetic acid each well on the orbital shaker for 15 min (100 rpm/min). Quantification was done through the method of measuring the OD values at 550 nm of the solution. All assays were performed in triplicate from at least three different experiments.

We also evaluate the lactic acid production and lactate dehydrogenase activity (LDH) of biofilm. Mature biofilms were washed gently twice with PBS, followed by stained with 1.5 mL BPW in each well for 3 h. The supernatant was collected and determined by lactic acid content detection kit (Solarbio, Beijing). The LDH activity of biofilm was washed and determined by LDH activity detection kit (Solarbio, Beijing). Meanwhile, the CFUs of biofilm were detected. The 24-h biofilm was gently cleaned twice with PBS, 1 mL of BHI was added to each hole and biofilms were scraped and blown to mix. Then they were diluted 10^1–10^{10} times, each concentration was coated with 100 μL bacterial solution. Count after 24 h culture under the same conditions. All assays were performed in triplicate from at least three different experiments.

Exopolysaccharide measurements

Anthrone–sulfuric acid colorime tric assay was applied to measure the amounts of WIG and WSG [20]. The method of biofilm formation and preparation has been described above. Biofilms were collected by scraping with same volume of deionized water and were centrifuged (4000 rpm, 4°C, 15 min) then WIG and WSG were isolated and were contained in supernatant and precipitate, respectively. The supernatant was filtered through a 0.22 μm pore size filter membrane (Corning Incorporated, USA) and separated for WSG measurement using the anthrone method. WIG was obtained by adding 1 M NaOH to the precipitated and incubating them on the orbital shaker (37°C, 3 h) then centrifugating (4000 rpm, 4°C, 15 min) and collecting the supernatant, which also needed filtered. For EPS assessment, 200 μL of soluble suspension was mixed with 600 μL of anthrone reagent. The mixtures were heated at 95°C for 10 min and cooled on ice. The absorbance of each sample at 625 nm was measured using a microplate reader (Gene Co., China). The corresponding polysaccharide concentration was calculated according to a prepared standard curve with a glucose standard (Figure S1). The exopolysaccharide was further purified for GPC and GC-MS assays. For

grown in BHIS at 37°C anaerobically and were monitored every 4 hours (h); (e) the biofilm growth of *S. mutans* obtained from crystal violet assay experiments revealed the AS*vicK* strain caused a reduction in biofilm formation. The results were averaged from 8 independent cultures of different strains (UA159, AS*vicK*, and SmuvicK+), and experiments were performed in triplicate ($n = 3$; *: $p < 0.05$); (f) the capacity of lactic acid production of biofilm were determined. The AS*vicK* strain had the lowest capacity of lactic production. The results were averaged from 8 independent cultures of different strains (UA159, AS*vicK*, and SmuvicK+), and experiments were performed in triplicate ($n = 3$; *: $p < 0.05$); (g) LDH activity were determined which revealed that the AS*vicK* strain had the lowest activity ($n = 3$; *: $p < 0.05$); (h) SEM of biofilms of UA159, AS*vicK*, and SmuvicK+ cultured in BHI supplemented with 1% sucrose. The AS*vicK* strain lower amounts of bacteria and EPS and looser biofilm structure. The yellow arrows represent bacteria while the red arrows represent EPS; (i) LDH activity/CFU were determined which revealed that the AS*vicK* strain had the lowest activity ($n = 3$; *: $p < 0.05$); (j) Lactic acid production/CFU of biofilm were determined. The AS*vicK* strain had the lowest capacity of lactic production ($n = 3$; *: $p < 0.05$).

GPC, using dextran as a standard, deionized water was added to prepare a solution to be tested with a concentration of about 5 mg/mL, and the loading volume is 20 μL. Column BRT105-104-102 tandem gel column (Borui Saccharide, China) was used for detection, and a standard curve was drawn according to the molecular mass (Mw) and retention time (RT) of standard sugars. WSG and WIG of UA159, AS*vicK* and SmuvicK+ were weighed and prepared into a 5 mg/mL solution. Centrifuge them at 12,000 rpm for 10 min. The supernatant was filtered with a 0.22 μm microporous membrane. The purity and relative molecular mass of the polysaccharide were measured. The molecular weight was calculated according to the standard curve. The monosaccharide analysis was done via GC-MS (ICS5000, ThermoFisher, USA) which is equipped with the chromatographic column (DionexCarbopacTMPA20, ThermoFisher, USA) (Appendix Figure A3). All assays were performed in triplicate from at least three different experiments.

Protein extraction for Western blotting and enzyme activity test

Mature biofilms were washed and collected in PBS. The precipitate was added with 500 μL of RIPA while the walls of cells were broken by freezing grinding apparatus (TuoHe, China). For Western blot assays, after centrifugating (14,000 ×*g*, 1 min, 4°C) and collecting the supernatant, protein concentrations were measured with Pierce BCA Protein Assay Kit (ThermoFisher Scientific, USA). Total proteins were stained using Commassie Blue Fast Staining Solution (Beyotime Biotechnology, China) to determine equal lane loads [33]. Same amounts of protein (20 μg) with 5 × SDS-PAGE Sample Loading Buffer (Bio-Rad, USA) were boiled for 10 min and loaded on gels to be fractionated. After being semi-dry electro-transferred to PVDF membranes (Thermo Scientific, USA) and blocked in 5% (w/v) non-fat dry milk at room temperature for 2 h. For measurement of VicK and Rnc, membranes were incubated with monoclonal antibodies (MAbs): anti-VicK and anti-Rnc (1:500, AbMax Biotechnology, Beijing, China) for incubation overnight at 4°C. Then membranes were washed in Tris-buffered saline containing 0.1% Tween 20, pH 7.5 and incubated with goat anti-rabbit secondary antibody conjugated with horseradish peroxidase (dilution 1:10000) at room temperature for 2 h. Protein signals were detected with the Immobilon Western Chemiluminescent HRP substrate kit (Millipore, USA) and determined the signal density with A BioRad GS-700 Imaging Densitometer. The enzyme activity of Gtfs was detected by zymogram analysis. planktonic bacteria were centrifugated (13000 rpm, 10 min, 4°C) and harvested. The supernatant was filtered by a 0.22 μm filter (Millipore, USA) and added 10 mL anhydrous ethanol for each 30 mL supernatant, then it was freezed at −80°C for 30 min. The precipitation was collected by centrifugation (25000 rpm, 15 min, 4°C) with PBS and protein concentrations were measured with Pierce BCA Protein Assay Kit (ThermoFisher Scientific, USA). Same amounts of protein (20 μg) with 5 × SDS-PAGE Sample Loading Buffer (Bio-Rad, USA) were boiled for 10 min and loaded on gels to be fractionated. One SDS-PAGE gel was placed in Coomassie bright blue dyed for 1 h, then placed in double distilled water overnight shaking at room temperature. The other was washed by phosphate buffer containing 2.5% TritonX-100 twice for 15 min and incubated in phosphate buffer containing 0.2% glucan T70 and 5% sucrose (pH = 6.5) at 37°C for 18 h. Rinse twice with double distilled water for 10 min. Then the white bands on SDS-PAGE glue were observed in a dark room [18].

Production of recombinant Rnc and RNase III activity assays

E. coli carrying the *rnc* recombinant plasmid was incubated in 5 mL LB medium containing ampicillin (50 μg/mL) for 16–18 h (150 rpm, 37°C). Then bacterial solution was diluted in 40 mL LB medium with 1 mM IPTG at a ratio of 1:20 and incubated at 37°C for about 3–4 h (OD600 = 0.5). The bacteria were centrifugated at 4°C (4000 rpm, 20 min, 4°C) and added 2 mL non-denaturing Lysis Buffer. Place them in ice for 30 min with lysozyme (1 mg/mL). The bacteria were lysed by ultrasound on ice and the supernatant was collected after centrifugated (4000 rpm, 20 min, 4°C). The column of BeyoGold™ HisTag Resin had been processed twice by non-denaturing lysate. The bacterial lysate was added to the resin and placed on the shaker for 3–4 h at 4°C. The column was washed 5 times with non-denaturing detergent. The solution was eluted 6–10 times with 0.5 mL of non-denaturing eluent. The eluent containing Rnc recombinant protein was centrifuged in 3 kDa ultrafiltration tube (4000 rpm, 20 min, 4°C). And, 4 mL of 1 × dialysate (20 mM Tris-hcl, 0.1 M NaCl) was added and centrifuged (4000 rpm, 20 min, 4°C). After repeating that twice, added 2 mL 2 × dialysate with 50% glycerol and centrifuged. Protein sample was stored, and proteinase inhibitor cocktail (Sigma, Germany) was added at −80°C. Rnc recombinant protein was verified by Western blot. For RNase activity assays, total RNAs were extracted from the UA159, AS*vicK* and SmuvicK+ strains and purified as previously described. Equal amounts of RNA (2 μg) were incubated with 4 nM of recombinant Rnc in 20 μL interaction buffer (10 mM Tris-HCl, pH = 8.0) for 30 min at 37°C. The mixtures were assessed by agarose gel electrophoresis.

RNA-Seq performance and statistical analysis of RNA-seq data

Strains of UA159 and AS*vicK* were incubated anaerobically at 37°C in BHI for 14–16 h. Then, they were diluted in 80 mL freshly prepared BHI medium at 1:20 volume and were incubated under the same conditions for 2.5–3 h. Centrifugation was performed (4000 rpm, 20 min, 4°C) and the supernatant was discarded. The bacteria with PBS buffer was washed and precipitated twice. Flash-frozen the bacteria in liquid nitrogen and then transferred them to −80°C for storage. RNA extraction and RNA-Seq were performed by the NextGen DNA Sequencing Core Laboratory of Majorbio Biotechnology Research (Shanghai, China). Reads were mapped to the genome of *S. mutans* UA159 (https://www.ncbi.nlm.nih.gov/genome/?term=AE014133). The sequencing result was uploaded on the website of NCBI, Accession: SRX18394998-SRX18395003. The classification and percentage of the DEGs were analyzed according to their functional annotations. Gene Ontology (GO) terms were assigned to genes using the DAVID tool [30]. Relative enrichment (overrepresentation) of GO terms for upregulated genes compared to a background of GO terms for all genes was assessed using Fisher's exact tests. In addition, a false discovery rate (FDR) procedure was used to correct for multiple hypothesis testing (FDR <0.05).

Immunoprecipitation analyses

Refer to lei et al.'s method of detecting post-transcriptional level regulation mechanism of asRNA using Co-IP experiment [20], the overexpressed AS*vicK* strain with HIS tag was cultured overnight and was diluted 20-fold into BHI and grown for 2.5–3 h to mid-logarithmic phase. After centrifugation (4000 rpm, 20 min, 4°C), the bacterial precipitation was collected and was washed with sterile PBS twice. Then, 500 μL of pre-cooled Lysis/Wash Buffer (Enhanced) (ACE Biotechnology, China) was added and mixed solution was incubated on ice for 5 min. The supernatant was collected after centrifugation (13000 ×*g*, 10 min, 4°C).

After rinsing the magnetic beads, 2–10 μg of antibody was added. The mixture was spined and incubated for 30 min at room temperature. Then we used 1×Lysis/Wash Buffer to wash them twice. Five hundred microliters of cell lysate (the total protein amount of 500 μg) was added to the centrifuge tube. The mixture was incubated at room temperature for 30 min and washed twice. Then, 50 μL of 1×SDS-PAGE Sample Loading Buffer (Bio-Rad, USA) was added to the centrifuge tube and heated at 100°C for 10 min. Magnetic beads were separated, and loading buffer containing target antigen was retained for RT-qPCR and Western blotting.

Examination of the ASvicK strain in vivo for plaque formation and cariogenic potential

Animal experiments were reviewed and approved by the Ethics Committee of the Affiliated Hospital of Stomatology Chongqing Medical University, ChongQing, China (Number of permit: (2022)126). Specific-pathogen-free (SPF), caries-susceptible 40 (half male and half female) Sprague-Dawley (SD) rats aged 21 days were used to investigate *in vivo* effects of UA159, AS*vicK* and SmuvicK+ strains on the formation of dental plaque, as well as cariogenic potential by SEM, CLSM and Keyes score. Rats were raised (Laboratory Animal Facility of the Affiliated Hospital of Stomatology Chongqing Medical University, Chongqing, China) and randomized into four groups: UA159 as a positive control, AS*vicK* group, SmuvicK+ group, and a blank group, which served as the negative control ($n = 10$ rats per group, half male and half female). On day 21 after birth, sterile water supplemented with 0.1% Ampicillin and food were available. On day 25, swabs were taken from the oral cavities of each rats to confirm that the endogenous streptococcus had been suppressed by diluted and plated the solution onto MSA supplemented with 0.2 U/mL bacitracin (Sigma Chemical Co., St Louis, USA). On days 26, each rat began to be infected orally using 200 μL of a bacterial suspension that comprised the UA159 strain, the AS*vicK* strain, the SmuvicK+ strain for a week. One week after association with bacterial strain, dental plaque was collected from the buccal surfaces of mandibular molars and extracted the biofilm DNA. After PCR amplification with specific primers (Appendix Table 3), the samples were determined colonization of *S. mutans* successfully by 1% agarose gel electrophoresis (Appendix Figure 4). To support the implantation of these bacteria, drinking water containing 5% sucrose and high-cariogenic diet 2000 (consisting of 28% skim milk, 15% powdered sucrose, 49% wheat flour, 5% brewer's yeast, 2% gevral protein, and 1% sodium chloride) were served to all rats after began to infect them. Rats were weighed once a week and their physical appearance was routinely recorded. On day 53 (at the end of the 32-day experimental period), the animals were sacrificed by CO_2 asphyxiation. Mandible with teeth, after being washed with PBS twice and immersed in 4% paraformaldehyde for 4 h lucifugally followed by 0.4% murexide for 6 h, were dissected into two pieces from mesial side to distal side. The teeth were observed under a stereomicroscope to observe smooth surface and fissure carious lesions. Meanwhile, they were scored according to a modified Keyes score [20,34]. We referred to the SEM and CLSM experimental methods in other experiments [20,35]. EPS matrix of dental plaque on the tooth surface was stained with 1 μM Alexa Fluor 647-labeled dextran conjugate (Life Tech, USA), and bacterial cells were labeled with 50 μL Syto9 Nucleic Acid Stain (Life Tech, USA).

Data analysis

Statistical analyses of the data were performed using SPSS 16.0 (SPSS Inc., Chicago, IL, USA). The Shapiro–Wilk test demonstrated whether the data were normally distributed, whereas Bartlett's test was used to assess the homogeneity of variances. For parametric testing, one-way ANOVA was used to detect the significant effects of variables followed by the Student–Newman–Keuls test to compare the means of each group. For non-parametric testing, the Kruskal–Wallis test and least significant difference (LSD) multiple comparisons were used. A value of $p < 0.05$ was considered significant.

Results

ASvicK altered structrue and growth of bacteria and biofilm

The morphological structure of the bacteria was examined under microscope and SEM. Typically, the Longer chain and diverse shape were apparent for the AS*vicK* strain in comparison with UA159 strain (Figure 1a, b). Growth curve and CFU curve of the AS*vicK* strain had a significantly extended lag phase compared with those of the UA159 strain illustrated that overexpression of AS*vicK* caused growth delay (Figure 1c, d). CV assay results showed that the biomass of the AS*vicK* strains was significantly decreased compared with the UA159 strain (Figure 1e). Lactic acid production and LDH activity revealed that AS*vicK* could diminish lactic acid metabolism (Figure 1f, g). At the same time, LDH activity/CFU and lactic acid production/CFU of AS*vicK* decreased, that mean its ability to produce acid was weakened (Figure 1i, j). Furthermore, the structure of biofilm was obtained using SEM displayed that the AS*vicK* strain had looser biofilm and less EPS (Figure 1h). These results demonstrated that the overexpression of the AS*vicK* led to the alteration of bacterial structure and reduction of bacterial growth and biofilm formation.

ASvicK inhibits EPS production and architecture of biofilm

The three-dimensional structure of biofilm was obtained using the CLSM. In contrast with the UA159 and SmuvicK+ strain, the AS*vicK* strain had less bacteria and EPS (Figure 2a). Meanwhile, overexpression of the AS*vicK* gene markedly decreased the production of WIG and WSG measured by anthrone–sulfuric acid colorime tric assay (Figure 2b). Determination of monosaccharide fractions by GC-MS revealed that the polysaccharide comprised glucose (Glc), galactose (Gal), arabinose (Ara) and fructose (Fru) with various molar ratios. The percentage of glucose in WIG of AS*vicK* strain was significantly decreased (Figure 2c). The molecular weight of exopolysaccharides of *vicK* mutant was analysed by GPC. The results showed that the molecular weight of EPS in the AS*vicK* strain was higher than the UA159 (Figure 2d).

ASvicK alters genes and enzymatic activity related to exopolysaccharide metabolism

S. mutans UA159 and the AS*vicK* strain were collected for the transcriptome analysis 325 differentially expressed genes (DEGs) with 159 genes upregulated and 166 genes downregulated in the AS*vicK* mutant were shown (Figure 3a). According to the NCBI *S. mutans* genome annotation, the function of the majority of the DEGs are unknown. And those with known functions were mainly associated with some processes (Figure 3a). The DAVID tool was used to better condense the gene function. In GO terms, downregulated genes primarily belong to the carbohydrate transport system (Figure 3b). The data from the transcriptome analysis was confirmed by RT-qPCR. The data of RT-qPCR indicated that overexpression of AS*vicK* transcript, compared to UA159, led to downregulation of the *gtfB*/*C*/*D* and *ftf* genes related to EPS synthesis (Figure 3c). The expression of *lacA*/*B*/*C*/*D*/*E*/*G*/*R* and *galK*/*T* genes related to lactose and galactose metabolism showed higher than that in UA159 strain (Figure 3d). In addition, the enzyme activity of Gtfs was significantly decreased in the AS*vicK* strain, while it was increased in the SmuvicK+ strain compared to the UA159 strain (Figure 3e).

ASvicK regulates the expression of vicK on post-transcriptional level

The amount of VicK and Rnc protein was reduced in the AS*vicK* strain which matched the RT-qPCR result (Figure 4a). To explore the post-transcriptional regulation of *vicK* by AS*vicK*, we produced and purified the RNase III, and the RNase III activity assays confirmed that the total RNAs could be degraded by RNase III, where the total mRNA degradation of AS*vicK* strain was more pronounced (Figure 4b). For further research, co-ip assay was adopted, which is an effective method to study the interaction between RNA and protein precipitation *in vivo*. We attached a His-tag to the end of AS*vicK* and used the principle of specific binding of anti-his antibody to his-tag antigen to explore the complex that binds to AS*vicK* in bacterial lysate. In this way, the relevant regulatory mechanism of

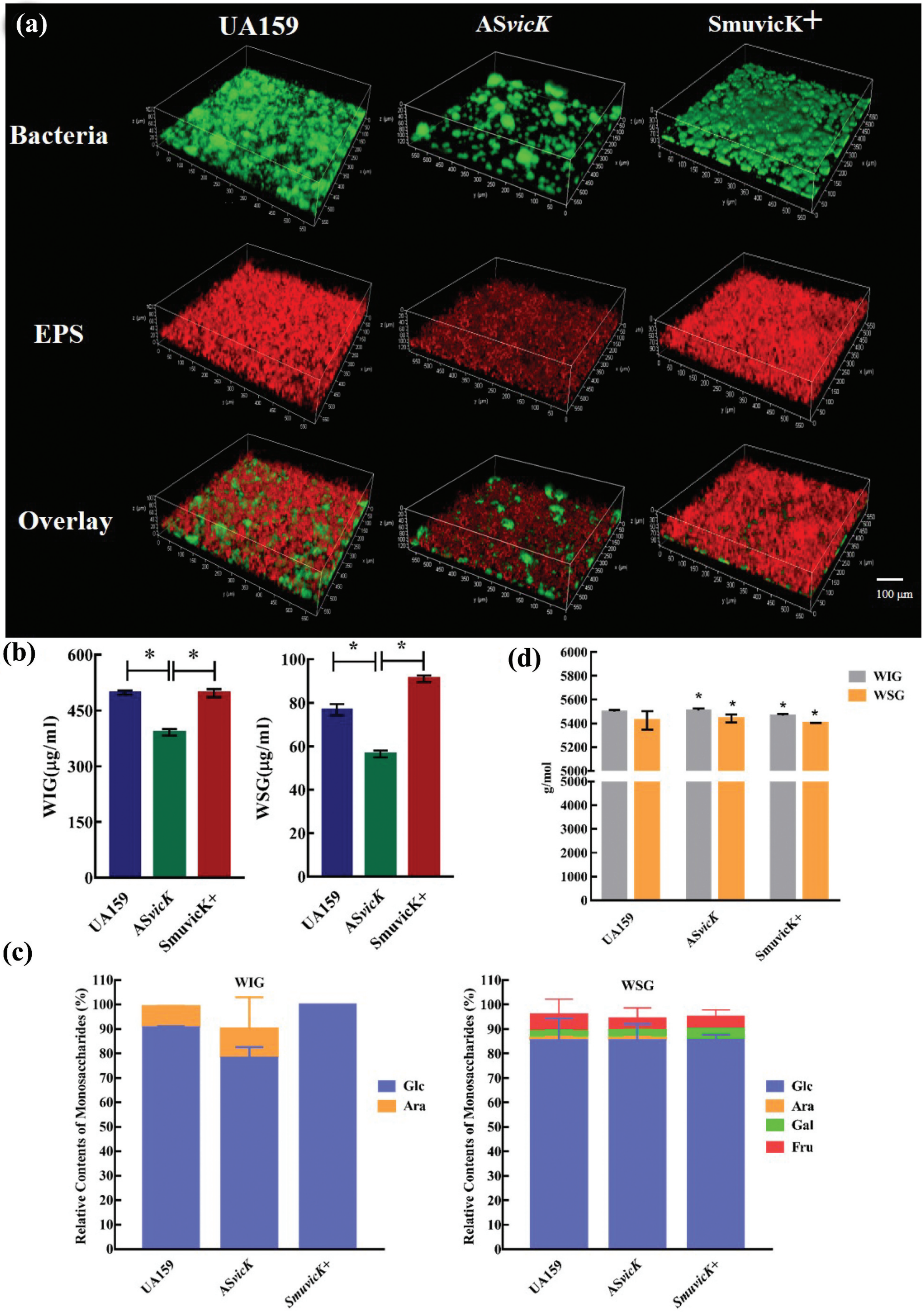

Figure 2. AS*vicK* inhibits EPS production *in vitro*. (a) CLSM of biofilms of UA159, AS*vicK*, and SmuvicK+ cultured in BHI supplemented with 1% sucrose. The AS*vicK* strain lower amounts of bacteria and EPS and looser biofilm structure and experiments were performed in triplicate; (b) Production of WIGs and WSGs of strains were measured by anthrone–sulfuric acid colorime tric assay. The results were averaged from 8 independent cultures of different strains (UA159, AS*vicK*, and SmuvicK +), and experiments were performed in triplicate ($n = 3$; *: $p < 0.05$); (c) a monosaccharide composition analysis of the polysaccharide was carried out. The results indicated the polysaccharide comprised Glc, Gal and Man with various molar ratios; (d) the molecular weight distribution of the polysaccharides of samples from different strains was estimated using GPC.

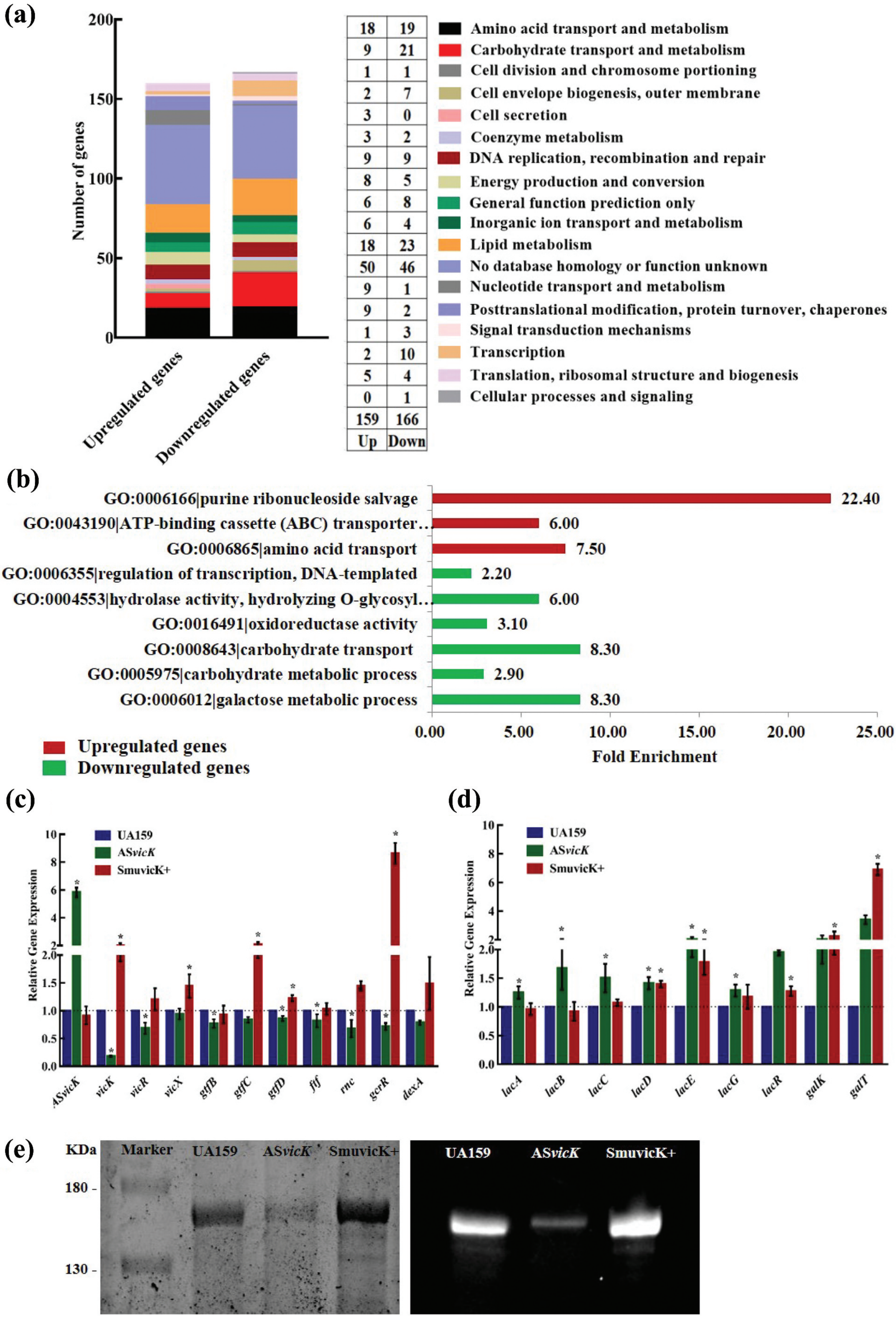

Up	Down
18	19
9	21
1	1
2	7
3	0
3	2
9	9
8	5
6	8
6	4
18	23
50	46
9	1
9	2
1	3
2	10
5	4
0	1
159	166

Figure 3. AS*vicK* alters genes and enzymatic activity related to exopolysaccharide metabolism. (a) the classification and percentage of the UA159 and the AS*vicK* strain DEGs were analyzed according to their functional annotations; (b) Gene ontology enrichment analysis of the DEGs using the DAVID tool. Upregulated genes are shown in red, and downregulated genes are shown in green; (c) RT-qPCR analysis showed the gene related to EPS metabolism transcripts in the UA159, AS*vicK*, and

AS*vicK in vivo* was explored. IP enriched 877 times by msRNA1657 was detected by RT-qPCR (Figure 4c). In addition, RNase III was co-iped with AS*vicK* indicated that AS*vicK* can enrich RNase III and form RNA–protein complex (Figure 4d).

AS*vicK* suppresses cariogenic pathogenicity *in vivo*

We verified a 1.76-fold increase in the expression of AS*vicK* in clinical strains screened from dental plaque of CF children and a 0.49-fold decrease of that in SECC children compared with the standard strain UA159 (Figure 5a). Next, we validated the effect of cariogenic pathogenicity of AS*vicK* in SD rats model. Rat molars of the lower dentition were observed under a stereomicroscope to determine the cariogenic severity according to Keyes Scores. We confirmed that the AS*vicK* group, similar with the blank control group, generated a lower cariogenic incidence in smooth and sulcal caries compared with the UA159 group (Figure 5b, c). The biofilms on the surface of molars were observed by SEM and CLSM (Figure 5d, E). We discovered the reduction of biofilms and EPS in the AS*vicK* group compared with the UA159 group. Besides, there was no significant difference in caries score or formation of biofilms and EPS between the SmuvicK+ group and the UA159 group.

Discussion

Inhibition of the synthesis of EPS, the main virulence factor of *S. mutans*, is an effective strategy for caries. In this study, we first found AS*vicK* RNA and demonstrated that AS*vicK* could inhibit bacterial growth and biofilm formation. AS*vicK* also affects production and composition of EPS on transcriptional and post-transcriptional levels, and ultimately attenuated cariogenesis of *S. mutans in vivo*.

In previous studies, we demonstrated that *rnc* gene interferes with extracellular polysaccharide metabolism and lactate production of *S. mutans* biofilms. Through the analysis of the transcriptome sequencing results of the *rnc* deletion strain, we first discovered AS*vicK* RNA. AS*vicK* can affect bacterial morphology (Figure 1a, b), which may be affected by genes related to cell wall synthesis and division. Slower bacterial growth in AS*vicK* mutants indicates that AS*vicK* has an inhibitory effect on the growth of *S. mutans* (Figure 1c, d). SmuvicK+ also showed growth defect, probably due to the interference of the introduction of the pDL278 recombinant plasmid with the VicRK system in regulating the homeostasis of *S. mutans* cells. The biomass and SEM observation of biofilm loosening further confirmed the inhibitory effect of AS*vicK* RNA on *S. mutans* biofilm formation (Figure 1e, h). The formation and stability of biofilm are closely connected with EPS. In this study, AS*vicK* had an impact on the content, structure and composition of EPS. The results of anthrone–sulfuric acid assay and CLSM indicated the decreased content of EPS and disintegrated three-dimensional structure of the biofilm of the AS*vicK* mutant (Figure 2a, b). Ulteriorly, we found the monosaccharide components with inhibited glucose and fructose and increased galactose in AS*vicK* strains (Figure 2c). The elevated molecular weight of EPS in the AS*vicK* group may be attributed to changes in the expression of polysaccharide metabolism genes that may alter the length of the glucan chain. The reduced composition ratio of glucose and the alterations of the glycosidic chain in the polysaccharide molecule may affect the structure of EPS, which may be the cause of the disintegration of the biofilm structure. The mechanisms of these phenomena need to be further explored.

Furthermore, lactic acid content and lactate dehydrogenase activity in the biofilm of AS*vicK* strain were decreased, as well as the lactic acid production and LDH activity of unit CFU of AS*vicK* strain, indicating that its ability to produce acid was weakened, which may be relevant to the inhibition of EPS. Bowen et al. proposed that EPS would lead to changes in biofilm permeability, thereby affecting the diffusion of lactic acid [4], which may be the reason for the reduced lactic acid content in the biofilm of AS*vicK* strain in this study. This hypothesis is supported by the report that EPS deficiency caused by *vicK* deletion reduces lactic acid production in *S. mutans* [36]. Another possibility is that AS*vicK* leads to decreased LDH activity and inhibits the conversion of pyruvate to lactate during glycolysis. Substrate alterations influenced by Lactic acid can dynamically regulate biofilm microecology, for example, *S. mutans* can inhibit *Streptococcus sanguinis* (*S. sanguinis*) and *Streptococcus gordonii* (*S. gordonii*) by producing lactic acid and other substances [37,38]. *Lactobacillus* can inhibit the growth and cariogenicity of *S. mutans* by producing lactic acid [39]. *Veillonella parvula* is a bacterium with lactic acid as carbon source, which can increase the expression of *S. mutans* Gtfs [40]. In this study, the

SmuvicK+ strains. *S. mutans* gene expression was relatively quantified by RT-qPCR using *gyrA* as an internal control ($n = 3$; *: $p < 0.05$); (d) RT-qPCR analysis showed the gene related to lactose and galactose metabolism transcripts in the UA159, AS*vicK*, and SmuvicK+ strains. *S. mutans* gene expression was relatively quantified by RT-qPCR using *gyrA* as an internal control ($n = 3$; *: $p < 0.05$); (e) the effect of AS*vicK* on GtfB/C/D enzymatic activity was verified by zymogram analysis.

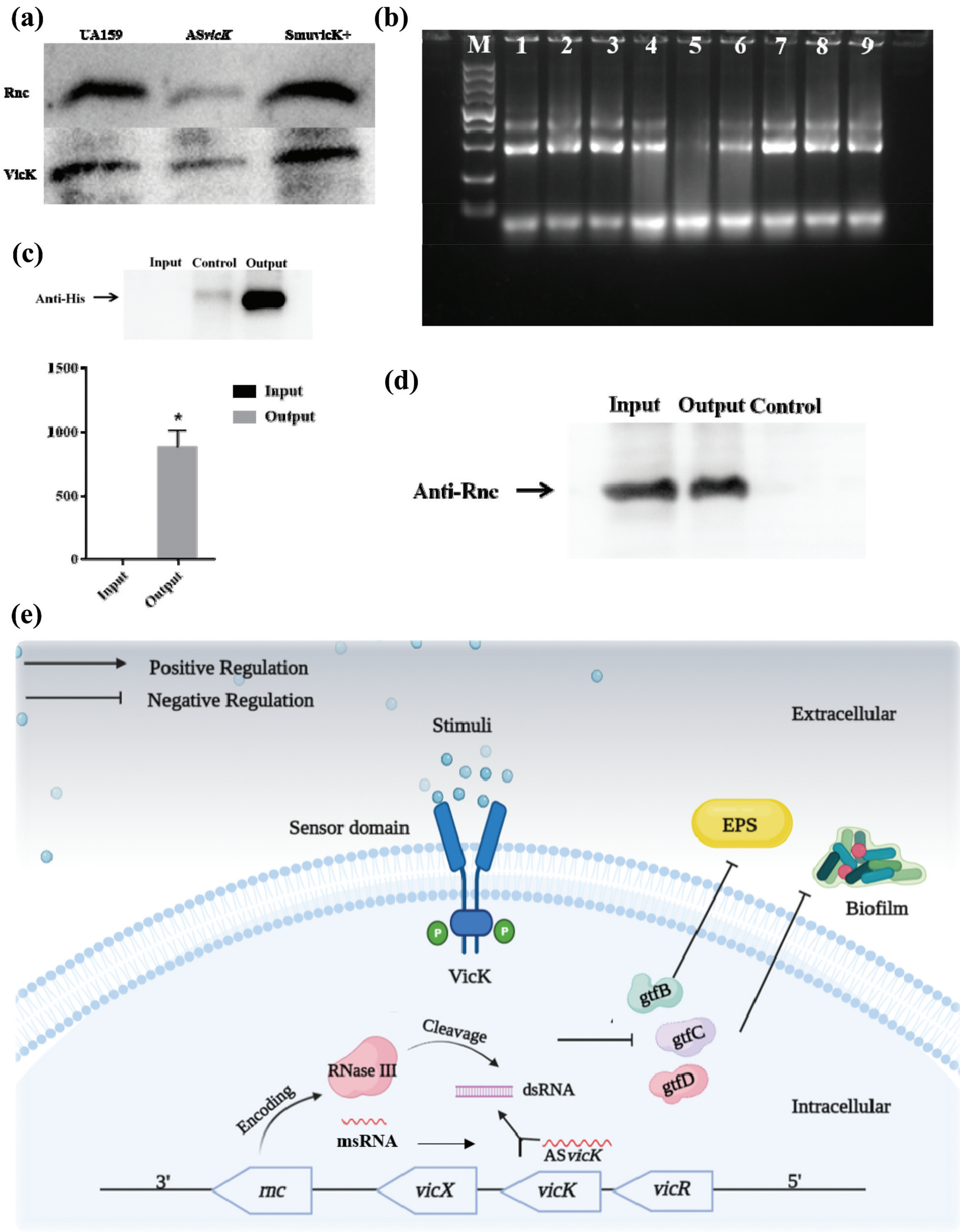

Figure 4. AS*vicK* regulates the expression of *vicK* on post-transcriptional level. (a) the production of VicK and Rnc was quantified by Western blotting in the cells grown; (b) Production of recombinant Rnc and RNase III activity assays. Equal amounts of RNA (2 µg) were incubated with 4 nM recombinant Rnc in 20 µL interaction buffer (10 mM Tris-HCl, pH 8.0) for 30 min at 37°C. For controls, equal amounts of RNA (2 µg) were incubated in 20 µL interaction buffer (10 mM Tris-HCl, pH 8.0) for 30 min at 37°C. M: Marker; Lane 1: UA159 total RNA + reaction mixture; lane 2: AS*vicK* strain total RNA + reaction mixture; lane 3: SmuvicK+ strain total RNA + reaction mixture; lane 4: UA159 total RNA + recombinant Rnc; lane 5: AS*vicK* strain total RNA+ recombinant Rnc; lane 6: SmuvicK+ strain total RNA+ recombinant Rnc; lane 7: UA159 total RNA; lane 8: AS*vicK* strain total RNA; lane 9: SmuvicK+ total RNA; (c) the post-transcriptional regulation mechanism of AS*vicK* was detected by co-ip. The expression of msRNA1657 was detected by RT-qPCR; (d) the expression of RNase III was detected by co-ip. AS*vicK* can enrich RNase III and form RNA-protein complex; (e) Working model of regulation by AS*vicK*.

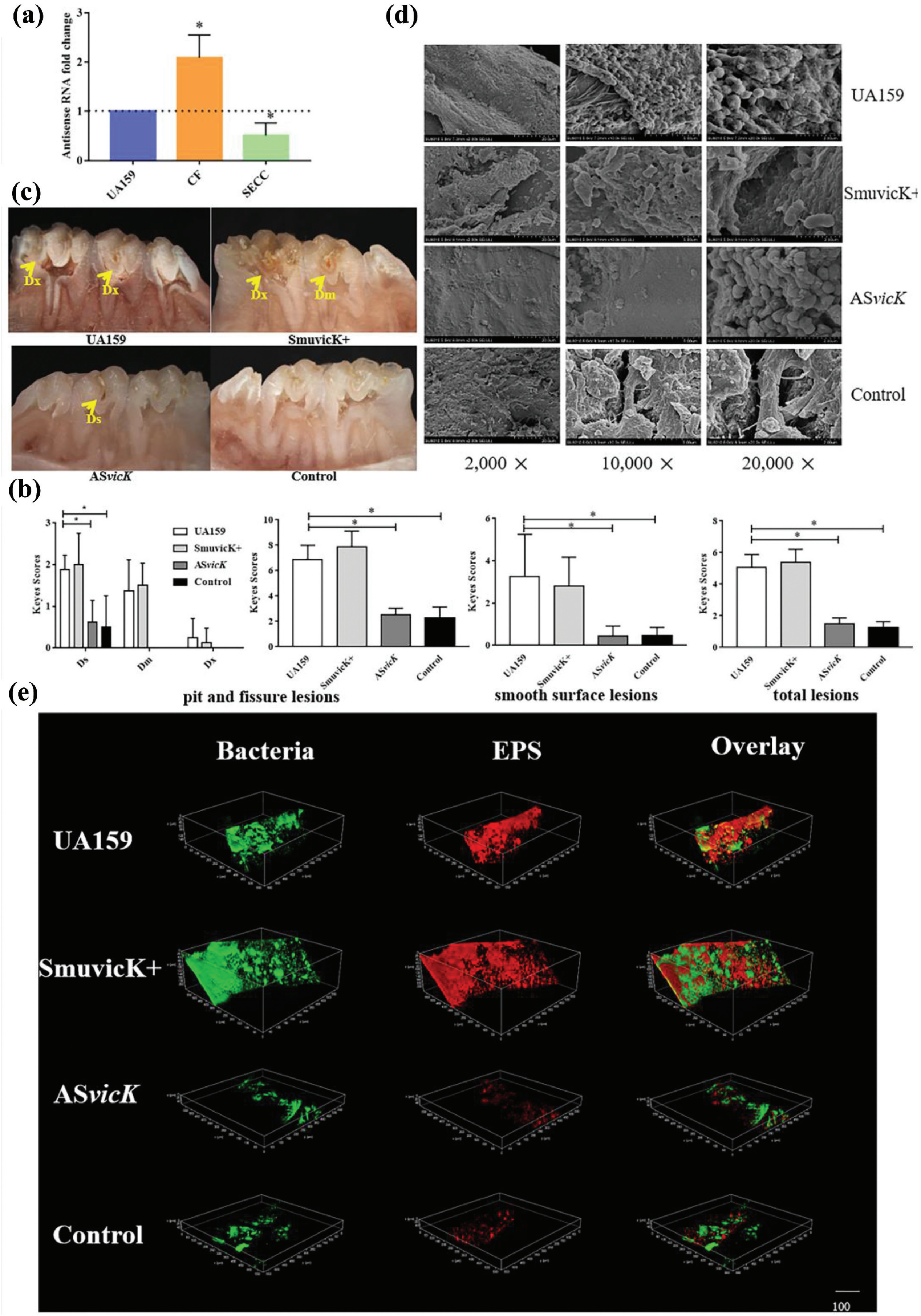

Figure 5. ASvicK suppresses cariogenic pathogenicity *in vivo*. (a) RT-qPCR analysis of ASvicK RNAs of clinical strains dental plaque from SECC children and CF children. *S. mutans* gene expression was relatively quantified by RT-qPCR and calculated based on UA159 expression set as 1.0 with *gyrA* as an internal control. Experiments were performed in triplicate and presented as the mean ± standard deviation; Shapiro–Wilk tests and Bartlett tests showed that the data were non-parametric. Significant

reduced production of lactic acid and the changed ratio of symbiotic biofilm bacteria with *S. sanguinis* and *S. gordonii* suggesting that AS*vicK* may transform the biofilm microecology from cariogenic state to non-cariogenic state by regulating the production of EPS and lactic acid (Appendix Figure 5).

Next, we explored the mechanism of AS*vicK* regulating biofilm and EPS formation. We found that overexpression of AS*vicK* generated impact on the EPS metabolism-related genes *gtfB*/*C*/*D*, *ftf* and *vicK*. Meanwhile, the ability to produce VicK protein and the enzyme activity of GTFs were diminished. Numerous studies have confirmed that VicK plays a crucial role in the biofilm formation of *S. mutans* and the expression of genes related to EPS metabolism [17,41]. Deletion of *vicK* results in down-regulation of *gtfD*, *ftf* and *gbpB* [35]. These studies are consistent with the results that down-regulation of the *vicK* gene in our AS*vicK* strain carried out decreased expression of *gtfB*/*C*/*D* and *ftf*. GTFs enzymatic activity was significantly reduced in AS*vicK* overexpressing strains, again confirming that AS*vicK* RNA affects EPS synthesis by affecting GTFs. In the previous results of GC-MS, the galactose fraction of AS*vicK* overexpressing strains increased. Lactose metabolism is mainly hydrolyzed into glucose and galactose-6-phosphate (Gal-6-P) through the tagatose pathway and LeIoir pathway [42,43], which is released from Lac-6-P. Glucose can be phosphorylated by galactokinase (GalK) before entering glycolysis [44,45]. In this study, the *lacA*/*B*/*C*/*D*/*E*/*G*/*R* genes involved in the lactose metabolism tagatose pathway and *galK* and *galT* gene expression was significantly increased. Therefore, lactose and galactose participate in the complex regulatory mechanism of EPS metabolism.

The changes in EPS metabolism-related genes were caused by the downregulated *vicK* gene generated by AS*vicK*. The *vicR*/*K*/*X* gene was co-located in operon 57 [46], the *vicR, vicX* and *gcrR* were down-regulated. Consistent with our results, it has reported that *gcrR*-deficient strains may impair acid production and cariogenicity. However, the difference is that *gcrR*-deficient strains have increased Gtfs expression and enhanced colonization ability [1,21,47]. In the presence of manganese, VicK can phosphorylate GcrR. Therefore, we speculate that the lack of biofilm and EPS is the result of complex regulation of AS*vicK* affecting multiple signal transduction systems at the transcriptional and/or translational level.

The reduction of *vicK* gene and protein in AS*vicK* strain preliminarily confirmed that AS*vicK* can effectively interfere with the transcription and translation of *vicK*. Still, its molecular mechanism remains obscure. We found that AS*vicK* forms an antisense complementary strand with the *vicK* gene while specifically adsorbing msRNA1657 and recruiting RNAse III to co-regulate the expression of *vicK* at both the transcriptional and post-transcriptional levels. Several studies have reported that RNase III can cleave the dsRNA formed by ASRNA and mRNA, providing evidence for this study [20,48]. The RNase III enzyme activity experiment proved that RNase III has the cleavage activity on AS*vicK*-mRNA, and achieves the purpose of rapidly regulating the expression of *vicK*. It has been reported that *rnc* mainly regulates the EPS decomposition-related gene [19,49]. In the AS*vicK* strain, *rnc* gene and associated protein are down-regulated, but the expression of *dexA* is reduced, taking into account the fact that most of the pathways regulating EPS in *S. mutans* are positive and complex. In addition, we predicted that AS*vicK* has a cyclic-like secondary structure (Appendix Figure 6). Circular RNA can specifically adsorb msRNA [19,20], further confirming that AS*vicK* can function by specifically adsorbing msRNA and RNase III. These results demonstrate that antisense RNAs and msRNAs regulate genes in multiple forms, reshape our understanding of bacterial gene regulation, and lay the foundation for exploring the regulatory mechanisms of AS RNAs in *S. mutans*.

In previous experiments, we confirmed that AS*vicK* inhibits formation of biofilm and EPS *in vitro*. In addition, the transcript level of AS*vicK* in the dental plaque of clinically caries-free children was significantly increased, suggesting that AS*vicK* is related to cariogenicity *in vivo*. Therefore, we further used an animal model of caries to simulate the interaction between the host, microbes and diet in the environment *in vivo*. We found that AS*vicK* inhibited EPS production by *S. mutans in vivo*, disrupted biofilm formation, and attenuated cariogenicity. Studies

differences were determined using the Kruskal–Wallis test and least significant difference (LSD) multiple comparisons method ($n = 8$; *: $p < 0.05$); (b) Keyes scores were used to calculate the pit and fissure caries, the smooth surface caries and total caries respectively in experimental rat. Shapiro-Wilk tests and Bartlett tests showed that the data were non-parametric. Significant differences were determined using the Kruskal–Wallis test and LSD multiple comparisons method ($n = 8$; *: $p < 0.05$); (c) the severity of pit fissure caries lesions of rat molars was observed under stereomicroscope; (d) SEM of biofilms on rat molars. Biofilm in the AS*vicK* group has significantly reduced EPS matrix similar to the blank control group, while the UA159 group and the SmuvicK+ group were covered with abundant EPS matrix; (e) Double labeling of biofilms on the tooth surface of rat molars. Green, total bacteria (SYTO 9); red, EPS (Alexa Fluor 647); scale bars, 100 µm. The AS*vicK* group has less bacteria and EPS matrix similar to the blank control group than the UA159 and SmuvicK+ group.

have reported that inactivation of *gtfB/C/D* can reduce the cariogenicity of *S. mutans* in vivo [50,51], and inactivation of the *gtfC* gene alone can reduce the adhesion of *S. mutans* to smooth surfaces [52]. In deficiency of *vick*, the ability of bacteria to acquire transduction signals is impaired, and the expression of *gtfB/C/D* genes is simultaneously affected, resulting in decreased biofilm formation and cariogenicity [35]. These studies support a reduction in the depth and severity of both smooth surface caries and pit and fissure caries in the AS*vicK* overexpression group. SEM and CLSM further confirmed that the compact structure of the biofilm in the AS*vicK* overexpression group was destroyed, and the content of EPS was reduced. Taking all these into consideration, we can reach the conclusion easily that *in vivo*, AS*vicK* inhibits the expression of adhesion-related genes by interfering with the expression of *vicK*. Synthesis of EPS reduces significantly, followed by destroyed structure of biofilm and reduced cariogenicity.

This study confirmed that AS*vicK* regulates *vicK* at the transcriptional and post-transcriptional levels, effectively inhibits EPS synthesis and biofilm formation, and reduces its cariogenicity *in vivo*. However, there are still some limitations. First of all, EPS is mainly glucan, but other polysaccharides that were less studied here also play a certain role in the cariogenic process. It is necessary to further explore the possible effects of AS*vicK* on fructose, galactose and other polysaccharides. Second, this study only explored the effect of AS*vicK* on a single species of *S. mutans*, while the dental plaque biofilm in the oral cavity is a habitat for a variety of bacteria, and the interaction of multiple microorganisms affects the balance of the microecology. For example, Gtfs can bind to oral microbes such as *Lactobacillus* and *Candida albicans* (*C. albicans*), affecting their EPS production [53,54] and enhancing the cariogenicity of symbiotic biofilms [55]. The vesicles of *S. mutans* containing Gtfs can also increase *C. albicans* biofilm formation by increasing EPS production [56,57]. *S. mutans* and oral *Streptococcus* mutually inhibit the growth of each other. The changes in the proportion of bacteria in the symbiotic biofilm of AS*vicK* strain, *S. sanguinis* and *S. gordonii* in the previous study also suggest that AS*vicK* may regulate the interaction between *S. mutans* and other oral microorganisms, and the mechanism needs to be further explored.

The caries prevalence of young children increases with age, the side effects and drug resistance of the currently used anti-caries methods cannot be ignored. Paying attention to the primary prevention of oral diseases and improving the comprehensive program of chronic disease prevention are the tasks that should be emphasized. Therefore, it is necessary to develop alternative inhibitors against the growth of *S. mutans* as a cariogenic bacterium. In this study, the AS*vicK* overexpressing strain showed weaker cariogenicity through a series of mechanisms, while ensuring the diversity of normal flora in the oral cavity, providing novel ideas and theoretical support for caries prevention and clinical work.

Disclosure statement

No potential conflict of interest was reported by the authors.

Funding

This research was funded by the National Natural Science Foundation of China under Grant Agreement (No. 31970783 and No. 32270888). This work was supported by a grant from National Science Fund for Distinguished Young Scholars (No. 82100991). This research was funded by the Top Talent Distinguished Professor from Chongqing Medical University [No. (2021) 215] and Program for Youth Innovation in Future Medicine from Chongqing Medical University (No. W0060). This research was funded by the Natural Science Foundation Project of Chongqing Science and Technology Commission (cstc2021jcyj-bshX0211) and the Basic Research and Frontiers Exploration Project of Science and Technology Committee of Yuzhong District (No. 20210124).

Author contributions

Y.T. Sun., H. Chen. and H.C. Mao. contributed to conception, design, data acquisition, analysis, and interpretation, drafted and critically revised the manuscript; S.Y. Yang., M.M. Xu. And X. Qiao., contributed to data acquisition, analysis, and interpretation, critically revised the manuscript; L.W. He., contributed to data acquisition and analysis, critically revised the manuscript; D.Q. Yang, contributed to conception, design, data acquisition, analysis, and interpretation, critically revised the manuscript. All authors gave final approval and agree to be accountable for all aspects of the work.

References

[1] Pan W, Mao T, Xu QA, et al. A new gcrR-deficient Streptococcus mutans mutant for replacement therapy of dental caries. ScientificWorldjournal. 2013;2013:460202.
[2] James SL, Abate D, Abate KH, et al. Global, regional, and national incidence, prevalence, and years lived with disability for 354 diseases and injuries for 195 countries and territories, 1990–2017: a systematic analysis for the Global Burden of Disease Study 2017. Lancet. 2018;392(10159):1789–1858. DOI:10.1016/S0140-6736(18)32279-7
[3] Karygianni L, Ren Z, Koo H, et al. Biofilm matrixome: extracellular components in structured microbial communities. Trends Microbiol. 2020;28(8):668–681.
[4] Bowen WH, Burne RA, Wu H, et al. Oral biofilms: pathogens, matrix, and polymicrobial interactions in

microenvironments. Trends Microbiol. 2018;26(3):229–242.
[5] Lin Y, Chen J, Zhou X, et al. Inhibition of Streptococcus mutans biofilm formation by strategies targeting the metabolism of exopolysaccharides. Crit Rev Microbiol. 2021;47(5):667–677.
[6] Koo H, Falsetta ML, Klein MI. The exopolysaccharide matrix: a virulence determinant of cariogenic biofilm. J Dent Res. 2013;92(12):1065–1073.
[7] Cugini C, Shanmugam M, Landge N, et al. The role of exopolysaccharides in oral biofilms. J Dent Res. 2019;98(7):739–745.
[8] Welin J, Wilkins JC, Beighton D, et al. Effect of acid shock on protein expression by biofilm cells of Streptococcus mutans. FEMS Microbiol Lett. 2003;227(2):287–293. DOI:10.1016/S0378-1097(03)00693-1
[9] Guo L, McLean JS, Lux R, et al. The well-coordinated linkage between acidogenicity and aciduricity via insoluble glucans on the surface of Streptococcus mutans. Sci Rep. 2015;5(1):18015.
[10] Wexler DL, Hudson MC, Burne RA. Streptococcus mutans fructosyltransferase (ftf) and glucosyltransferase (gtfBC) operon fusion strains in continuous culture. Infect Immun. 1993;61(4):1259–1267.
[11] Matsumoto M, Fujita K, Ooshima T. Binding of glucan-binding protein C to GTFD-synthesized soluble glucan in sucrose-dependent adhesion of Streptococcus mutans. Oral Microbiol Immunol. 2006;21(1):42–46.
[12] Smith DJ. Dental caries vaccines: prospects and concerns. Crit Rev Oral Biol Med. 2002;13(4):335–349.
[13] Bowen WH, Koo H. Biology of Streptococcus mutans-derived glucosyltransferases: role in extracellular matrix formation of cariogenic biofilms. Caries Res. 2011;45(1):69–86.
[14] Villanueva M, Garcia B, Valle J, et al. Sensory deprivation in Staphylococcus aureus. Nat Commun. 2018;9(1):523. DOI:10.1038/s41467-018-02949-y
[15] Dobihal GS, Brunet YR, Flores-Kim J, et al. Homeostatic control of cell wall hydrolysis by the WalRK two-component signaling pathway in Bacillus subtilis. Elife. 2019;8. DOI:10.7554/eLife.52088
[16] Kong L, Su M, Sang J, et al. The W-Acidic motif of histidine kinase walk is required for signaling and transcriptional regulation in streptococcus mutans. Front Microbiol. 2022;13:820089.
[17] Senadheera MD, Guggenheim B, Spatafora GA, et al. A VicRK signal transduction system in Streptococcus mutans affects gtfBCD, gbpB, and ftf expression, biofilm formation, and genetic competence development. J Bacteriol. 2005;187(12):4064–4076. DOI:10.1128/JB.187.12.4064-4076.2005
[18] Lei L, Yang Y, Mao M, et al. Modulation of biofilm exopolysaccharides by the streptococcus mutans vicX gene. Front Microbiol. 2015;6:1432.
[19] Mao MY, Yang YM, Li KZ, et al. The rnc gene promotes exopolysaccharide synthesis and represses the vicRKX gene expressions via microRNA-Size small RNAs in streptococcus mutans. Front Microbiol. 2016;7:687.
[20] Lei L, Zhang B, Mao M, et al. Carbohydrate metabolism regulated by antisense vicR RNA in cariogenicity. J Dent Res. 2020;99(2):204–213. DOI:10.1177/0022034519890570
[21] Khara P, Mohapatra SS, Biswas I. Role of CovR phosphorylation in gene transcription in Streptococcus mutans. Microbiology (Reading). 2018;164(4):704–715.
[22] Dunning DW, McCall LW, Powell WF, et al. SloR modulation of the Streptococcus mutans acid tolerance response involves the GcrR response regulator as an essential intermediary. Microbiology (Reading). 2008;154(Pt 4):1132–1143. DOI:10.1099/mic.0.2007/012492-0
[23] Millar JA, Raghavan R. Modulation of bacterial fitness and virulence through antisense RNAs. Front Cell Infect Microbiol. 2020;10:596277.
[24] Raghavan R, Sloan DB, Ochman H. Antisense transcription is pervasive but rarely conserved in enteric bacteria. MBio. 2012;3(4). DOI:10.1128/mBio.00156-12
[25] Lejars M, Caillet J, Solchaga-Flores E, et al. Regulatory interplay between RNase III and antisense RNAs in E. coli: the case of AsflhD and FlhD, component of the master regulator of motility. MBio. 2022;13(5):e0098122.
[26] Gordon GC, Cameron JC, Pfleger BF. RNA sequencing identifies new RNase III cleavage sites in Escherichia coli and Reveals Increased Regulation of mRNA. MBio. 2017;8(2). DOI:10.1128/mBio.00128-17
[27] Nicholson AW. Ribonuclease III mechanisms of double-stranded RNA cleavage. Wiley Interdiscip Rev RNA. 2014;5(1):31–48.
[28] Zhang Y, Xie X, Ma W, et al. Multi-targeted antisense oligonucleotide delivery by a framework nucleic acid for inhibiting biofilm formation and virulence. Nanomicro Lett. 2020;12(1):74. DOI:10.1007/s40820-020-0409-3
[29] Duque C, Stipp RN, Wang B, et al. Downregulation of GbpB, a component of the VicRK regulon, affects biofilm formation and cell surface characteristics of Streptococcus mutans. Infect Immun. 2011;79(2):786–796. DOI:10.1128/IAI.00725-10
[30] Ajdic D, McShan WM, McLaughlin RE, et al. Genome sequence of Streptococcus mutans UA159, a cariogenic dental pathogen. Proc Natl Acad Sci U S A. 2002;99(22):14434–14439. DOI:10.1073/pnas.172501299
[31] Bustin SA, Benes V, Garson JA, et al. The MIQE guidelines: minimum information for publication of quantitative real-time PCR experiments. Clin Chem. 2009;55(4):611–622. DOI:10.1373/clinchem.2008.112797
[32] Chen H, Zhang B, Weir MD, et al. S. mutans gene-modification and antibacterial resin composite as dual strategy to suppress biofilm acid production and inhibit caries. J Dent. 2020;93:103278.
[33] Lei L, Stipp RN, Chen T, et al. Activity of Streptococcus mutans VicR is modulated by antisense RNA. J Dent Res. 2018;97(13):1477–1484.
[34] Keyes PH. Dental caries in the molar teeth of rats. II. A method for diagnosing and scoring several types of lesions simultaneously. J Dent Res. 1958;37(6):1088–1099.
[35] Deng Y, Yang Y, Zhang B, et al. The vicK gene of Streptococcus mutans mediates its cariogenicity via exopolysaccharides metabolism. Int J Oral Sci. 2021;13(1):45. DOI:10.1038/s41368-021-00149-x
[36] Senadheera D, Krastel K, Mair R, et al. Inactivation of VicK affects acid production and acid survival of

Streptococcus mutans. J Bacteriol. 2009;191(20):6415–6424. DOI:10.1128/JB.00793-09
[37] Nicolas GG, Lavoie MC. Streptococcus mutans and oral streptococci in dental plaque. Can J Microbiol. 2011;57(1):1–20.
[38] Chen H, Yang Y, Weir MD, et al. Regulating oral biofilm from cariogenic state to non-cariogenic state via novel combination of bioactive therapeutic composite and gene-knockout. Microorganisms. 2020;8(9):1410.
[39] Wasfi R, El-Rahman OA A, Zafer MM, et al. Probiotic Lactobacillus sp. inhibit growth, biofilm formation and gene expression of caries-inducing Streptococcus mutans. J Cell Mol Med. 2018;22(3):1972–1983.
[40] Liu S, Chen M, Wang Y, et al. Effect of Veillonella parvula on the physiological activity of Streptococcus mutans. Arch Oral Biol. 2020;109:104578.
[41] Zhang Q, Ma Q, Wang Y, et al. Molecular mechanisms of inhibiting glucosyltransferases for biofilm formation in Streptococcus mutans. Int J Oral Sci. 2021;13(1):30.
[42] Zeng L, Das S, Burne RA. Utilization of lactose and galactose by Streptococcus mutans: transport, toxicity, and carbon catabolite repression. J Bacteriol. 2010;192(9):2434–2444.
[43] Morse ML, Hill KL, Egan JB, et al. Metabolism of lactose by Staphylococcus aureus and its genetic basis. J Bacteriol. 1968;95(6):2270–2274.
[44] Abranches J, Chen YY, Burne RA. Galactose metabolism by Streptococcus mutans. Appl Environ Microbiol. 2004;70(10):6047–6052.
[45] Calmes R. Involvement of phosphoenolpyruvate in the catabolism of caries-conducive disaccharides by Streptococcus mutans: lactose transport. Infect Immun. 1978;19(3):934–942.
[46] Podgornaia AI, Casino P, Marina A, et al. Structural basis of a rationally rewired protein-protein interface critical to bacterial signaling. Structure. 2013;21(9):1636–1647.
[47] Idone V, Brendtro S, Gillespie R, et al. Effect of an orphan response regulator on Streptococcus mutans sucrose-dependent adherence and cariogenesis. Infect Immun. 2003;71(8):4351–4360. DOI:10.1128/IAI.71.8.4351-4360.2003
[48] Huang L, Deighan P, Jin J, et al. Tombusvirus p19 captures RNase iii-cleaved double-stranded RNAs formed by overlapping sense and antisense transcripts in Escherichia coli. MBio. 2020;11(3):e00485–20.
[49] Mao MY, Li M, Lei L, et al. The regulator gene rnc is closely involved in biofilm formation in streptococcus mutans. Caries Res. 2018;52(5):347–358.
[50] Yamashita Y, Bowen WH, Burne RA, et al. Role of the Streptococcus mutans gtf genes in caries induction in the specific-pathogen-free rat model. Infect Immun. 1993;61(9):3811–3817.
[51] Ren Z, Cui T, Zeng J, et al. Molecule targeting glucosyltransferase inhibits Streptococcus mutans biofilm formation and virulence. Antimicrob Agents Chemother. 2016;60(1):126–135. DOI:10.1128/AAC.00919-15
[52] Tsumori H, Kuramitsu H. The role of the Streptococcus mutans glucosyltransferases in the sucrose-dependent attachment to smooth surfaces: essential role of the GtfC enzyme. Oral Microbiol Immunol. 1997;12(5):274–280.
[53] Ellepola K, Liu Y, Cao T, et al. Bacterial GtfB augments Candida albicans accumulation in cross-kingdom biofilms. J Dent Res. 2017;96(10):1129–1135.
[54] Noda M, Sugihara N, Sugimoto Y, et al. Lactobacillus reuteri BM53-1 produces a compound that inhibits sticky glucan synthesis by Streptococcus mutans. Microorganisms. 2021;9(7):1390.
[55] Souza JGS, Bertolini M, Thompson A, et al. Role of glucosyltransferase R in biofilm interactions between Streptococcus oralis and Candida albicans. Isme J. 2020;14(5):1207–1222. DOI:10.1038/s41396-020-0608-4
[56] Wu R, Cui G, Cao Y, et al. Streptococcus mutans membrane vesicles enhance Candida albicans pathogenicity and carbohydrate metabolism. Front Cell Infect Microbiol. 2022;12:940602.
[57] Wu R, Tao Y, Cao Y, et al. Streptococcus mutans membrane vesicles harboring glucosyltransferases augment Candida albicans biofilm development. Front Microbiol. 2020;11:581184.